# Dispersion curves

Milad Bader

This document is an edited extract from my Ph.D. research proposal.

# INTRODUCTION

Guided waves exhibit complex behavior due to the physical conditions fulfilled at the boundaries. They theoretically contain an infinite number of dispersive modes, in which only specific frequency-wavenumber pairs can sustain propagation. Lamb (1917) has extensively studied the case of elastic P-SV waves trapped in an infinite plate with free-surface boundary conditions. This configuration formed the basis for non-destructive evaluation techniques with applications in civil engineering for the assessment of near-surface rigid layers (Ryden and Lowe, 2004) and in medical imaging for defect evaluation of long bones (Rao et al., 2016; Vallet et al., 2016).

In exploration seismology, guided waves, like surface waves, are often treated as noise and removed from the data. On some occasions, surface waves are used to build near-surface S-wave velocity models via dispersion curves analysis (Aki and Richards, 2002). Following a similar analysis, interior guided waves, created by low-velocity zones in the shallow subsurface, can be used to characterize the near-surface in both onshore and offshore environments (Boiero et al., 2013; Hou et al., 2018). In coal mining, interior guided waves are used to detect faults in seams embedded between stiffer rocks (Krey, 1963). However, including guided waves in full-waveform inversion (FWI) in practical applications remains challenging. It requires an accurate elastic starting model, including S-wave velocity and density, even when only P-wave velocity is inverted. This requirement is due to the strong entanglement between the propagating eigenmodes and the boundary properties of their waveguide. In addition, smooth models will predict significantly different guided wave properties compared to a sharp structure. Li et al. (2018) uses a hybrid approach combining dispersion curves inversion and numerical wave propagation to build near-surface P-wave velocity model robustly. Dispersion curve analysis of normal and leaky modes allows building a layered model that can serve as a starting model for FWI.

Here, I introduce a general formulation to compute P-SV dispersion curves with different boundary conditions.

# GUIDED WAVES DISPERSION CURVES

In this section, I develop a general framework to compute P-SV dispersion curves in isotropic layered media. The framework handles different types of guided waves: surface waves, Lamb waves (known as plate waves), and stratified layers embedded between two half-spaces. It allows computing both normal and leaky modes dispersion curves. My final aim is to invert these curves and build starting models for elastic FWI.

## Building field and propagator matrices

For a horizontally layered medium depicted in Figure 1, I follow Thomson-Haskell method (Thomson, 1950; Haskell, 1953) and build the field matrix for each layer, then I combine them to deduce the whole system propagator matrix.

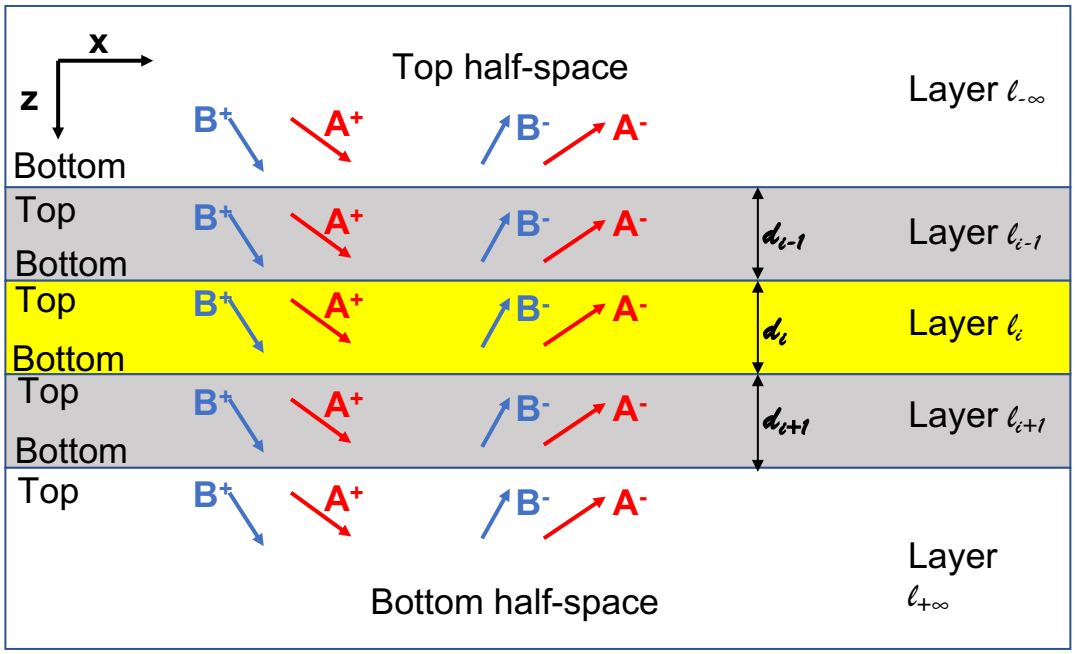


Figure 1: A sketch illustrating a horizontally layered medium. In each layer there are four plane waves: downgoing and upgoing P- and SV-waves.

For a homogeneous layer $l_i$, I seek plane wave solutions for the P-wave scalar potential field $\phi$ and the SV-wave vector potential field $(0, \psi, 0)^T$. These solutions satisfy the corresponding wave equations and have the form

$$\begin{aligned} \phi &= e^{i(kx-\omega t)}(A^+ e^{ikr_a z} + A^- e^{-ikr_a z}) \\ \psi &= e^{i(kx-\omega t)}(B^+ e^{ikr_b z} + B^- e^{-ikr_b z}) \ , \end{aligned} \tag{1}$$

with the following notations:

$$
\begin{aligned}
A^+, B^+ &\quad \text{amplitudes of downgoing waves.} \\
A^-, B^- &\quad \text{amplitudes of upgoing waves.} \\
k &\quad \text{horizontal wavenumber, can be a complex number.} \\
\omega &\quad \text{angular frequency} \\
\alpha, \beta &\quad \text{P- and S-wave speed} \\
c = \frac{\omega}{k} &\quad \text{phase velocity if } k \text{ is real.} \\
r_a = \sqrt{\frac{c^2}{\alpha^2} - 1} &\quad \text{can be a complex number.} \\
r_b = \sqrt{\frac{c^2}{\beta^2} - 1} &\quad \text{can be a complex number.}
\end{aligned}
$$

The state variables of interest are the displacements $u_x, u_z$ and the stress tensor components $\sigma_{xz}, \sigma_{zz}$ which are related to the potential fields by the equations

$$
\begin{aligned}
u_x &= \frac{\partial \phi}{\partial x} - \frac{\partial \psi}{\partial z} \\
u_z &= \frac{\partial \phi}{\partial z} + \frac{\partial \psi}{\partial x} \\
\sigma_{xz} &= \rho\beta^2 (2\frac{\partial^2 \phi}{\partial x \partial z} + \frac{\partial^2 \psi}{\partial x^2} - \frac{\partial^2 \psi}{\partial z^2}) \\
\sigma_{zz} &= \rho\alpha^2 \frac{\partial^2 \phi}{\partial z^2} + \rho(\alpha^2 - 2\beta^2)\frac{\partial^2 \phi}{\partial x^2} + 2\rho\beta^2 \frac{\partial^2 \psi}{\partial x \partial z} \ ,
\end{aligned}
\tag{2}
$$

where $\rho$ is the density in the layer $l_i$.

After some algebraic manipulation, the state variables can be expressed as a function of the amplitudes vector:

$$
\mathbf{v}_i = \mathbf{W} \cdot \mathbf{Q}_i \cdot \mathbf{E}_i(z) \cdot \mathbf{a}_i \ , \tag{3}
$$

where $\mathbf{v}_i = (u_x, u_z, \sigma_{xz}, \sigma_{zz})^T$, $\mathbf{a}_i = (A^+, A^-, B^+, B^-)^T$, $\mathbf{E}_i(z)$ is a diagonal matrix with the phase shift operators, $\mathbf{Q}_i$ is a matrix that depends on the properties of the layer $l_i$, and $\mathbf{W}$ is a diagonal matrix that depends on $k$ and the phase term $e^{i(kx-\omega t)}$. This decomposition is similar to the one given in Buchen and Ben-Hador (1996). I give in Appendix A the entries of these matrices. $\mathbf{W}$ is common to all layers in the system and does not affect the dispersion curves calculations, thus I omit it in the rest of the development.

I define the field matrix $\mathbf{D}_i(z) := \mathbf{Q}_i \cdot \mathbf{E}_i(z)$ that relates the amplitudes to the state variables in a given layer $l_i$ at depth $z$. I also define the propagator matrix $\mathbf{T}_i(z_2 - z_1) := \mathbf{Q}_i \cdot \mathbf{E}_i(z_2 - z_1) \cdot \mathbf{Q}_i^{-1}$ that relates the state variables at two different depths $z_1$ and $z_2$ in the same layer $l_i$. This matrix satisfies $\mathbf{T}_i^{-1}(z) = \mathbf{T}_i(-z)$ and

$\mathbf{T}_i(z_1 + z_2) = \mathbf{T}_i(z_1) \cdot \mathbf{T}_i(z_2)$. Each layer has its own depth origin $z = 0$ at its top boundary except for the top half-space that has the depth origin at its bottom. By using the continuity of state variables across interfaces between adjacent layers, I can relate the amplitudes or state variables between any two depth levels in the system using a single $4 \times 4$ matrix $\mathbf{M}$:

$$\mathbf{a}_j, \mathbf{v}_j = \mathbf{M} \cdot \mathbf{a}_k, \mathbf{v}_k \ . \tag{4}$$

The matrix $\mathbf{M}$ is merely the product of the appropriate $\mathbf{D}$ and $\mathbf{T}$ matrices (and their inverses). For illustration, I write the relation between the state variables at the top of layer $l_{i-1}$ and the amplitudes in the bottom half-space in Figure 1:

$$\begin{aligned} &\mathbf{a}_{+\infty} = \mathbf{M} \cdot \mathbf{v}_{i-1,top} \\ &\mathbf{M} = \mathbf{D}^{-1}_{+\infty}(0) \cdot \mathbf{T}_{i+1}(d_{i+1}) \cdot \mathbf{T}_i(d_i) \cdot \mathbf{T}_{i-1}(d_{i-1}) \ . \end{aligned}$$

This type of equations is used to compute surface waves dispersion curves as I will highlight in the next section.

## Dispersion characteristic functions

The dispersion characteristic function defines the relation that $\omega$ and $k$ must satisfy to allow the propagation of plane waves in the layered medium, given a certain set of boundary conditions. The relation is written in the form $f(\omega, k) = 0$ so that the computation of dispersion curves ($(\omega, k)$ pairs) amounts to finding the roots of $f$. Depending on the boundary conditions, I compute $f$ by taking the determinant of a $2 \times 2$ submatrix of $\mathbf{M}$.

*Surface waves*

For surface waves in a medium composed of $n$ layers overlying a half-space, the top half-space $l_{-\infty}$ is considered as void and the normal displacement and stress at its bottom must vanish. For modal solutions, no energy enters the system; the amplitudes of the upgoing waves in the bottom half-space $l_{+\infty}$ must also vanish. The general equation 4 reduces to

$$\mathbf{0} = \mathbf{M}[2, 4; 1, 2] \cdot \mathbf{v}_{1,top}[1, 2] \ , \tag{5}$$

where $\mathbf{M} = \mathbf{D}^{-1}_{+\infty}(0) \cdot \prod_{i=1}^{n} \mathbf{T}_i(d_i)$ and $\mathbf{v}_{1,top}[1, 2] = (u_x, u_z)^T_{1,top}$. The square bracket $[2, 4; 1, 2]$ designates the submatrix formed by the second and fourth rows, and the first and second columns. The characteristic function in this case is $f = \det(\mathbf{M}[2, 4; 1, 2])$.

*Lamb waves*

Lamb waves are P-SV waves trapped in an infinite free solid layer (or pile of layers). They have been extensively studied by Lamb (1917). Both half-spaces (top and bottom) are void and the normal displacements and stresses must vanish. The equation 4 for a $n$-layers plate becomes

$$\mathbf{0} = \mathbf{M}[3,4;1,2] \cdot \mathbf{v}_{1,top}[1,2] \ , \tag{6}$$

where $\mathbf{M} = \prod_{i=1}^{n} \mathbf{T}_i(d_i)$. The characteristic function is $f = \det(\mathbf{M}[3,4;1,2])$.

For a single layer, the modal solutions can be separated into symmetric and anti-symmetric modes depending on the displacement symmetry with respect to the center of the plate. This requires writing the plane wave solutions 1 as sum of symmetric and anti-symmetric functions instead of downgoing and upgoing waves, and working with the four boundary conditions explicitly (Viktorov, 1967). The formulation 6 does not allow this separation at the benefit of generality.

*Embedded layer*

For a layer (or pile of layers) embedded between two solid half-spaces, the model solutions are obtained by imposing that no energy enters the system. Thus, the amplitudes of the downgoing waves in the top half-space and those of the upgoing waves in the bottom half-space must vanish. The equation 4 for $n$ embedded layers writes

$$\mathbf{0} = \mathbf{M}[1,3;2,4] \cdot \mathbf{a}_{1,top}[2,4] \ , \tag{7}$$

where $\mathbf{M} = \mathbf{D}^{-1}_{+\infty}(0) \cdot \prod_{i=1}^{n} \mathbf{T}_i(d_i) \cdot \mathbf{D}_{-\infty}(0)$. The characteristic function is $f = \det(\mathbf{M}[1,3;2,4])$.

## Normal and leaky modes

Normal modes have amplitudes that decay in the direction orthogonal to the propagation. Leaky modes have amplitudes that decay in the propagation direction. In the configuration of interest, the propagation direction is horizontal and the attenuation due to leakage is caused by the radiation of waves into the top and bottom half-spaces. For a three-layer model, I show in Figure 2 a snapshot of the wavefield kinetic energy density ($\frac{1}{2}\rho|\dot{\mathbf{u}}|^2$). The normal waves (superposition of normal modes) propagate at a slower velocity and their amplitudes decay exponentially in the vertical direction into the top and bottom half-spaces. The leaky waves propagate at a higher velocity and they radiate energy into the half-spaces.

In the development above, I haven't specified if the matrices or the characteristic functions are related to normal or leaky modes. In fact, the general framework that

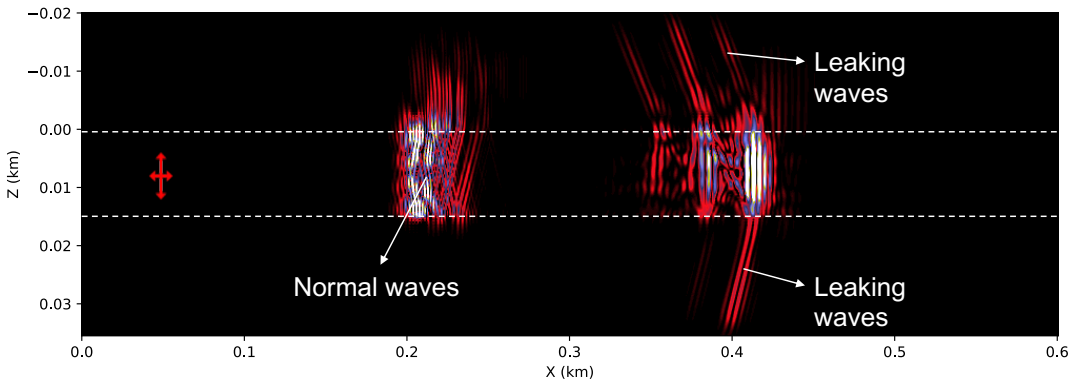


Figure 2: Snapshot of the wavefield kinetic energy density propagating in a three-layer model and excited by the source located at the red cross.

I described is applicable to both. The difference resides in the type of the horizontal wavenumber $k$. For normal modes, $k$ is real-valued. Without loss of generality, I consider only positive values for $k$ (propagation in the increasing $x$ direction). The characteristic function $f$ is still complex-valued *a priori*. However, its roots occur only on the real axis (of $f$). Therefore, I compute the dispersion curves for normal modes by finding the roots of $\Re(f(\omega, k))$.

As for the leaky modes, either the angular frequency $\omega$ or the horizontal wavenumber $k$ can be made complex-valued. I choose the second approach. In this case the real part $k_{re}$ defines the physical horizontal wavenumber (and the phase velocity), and the imaginary part $k_{im}$ defines the attenuation due to leakage. Both parts have to be positive. No simplification can be done to the characteristic function in this case and I compute the dispersion curves by finding the roots of $f(\omega, k_{re}, k_{im})$.

## Numerical aspects

*The large frequency-thickness problem*

A well-known limitation of the Haskell-Thomson method is the high-frequency (or large layer thickness) problem that leads to dramatic round-off errors when computing the characteristic function. To overcome this issue, I replace the matrices $\mathbf{D}$, $\mathbf{D}^{-1}$, and $\mathbf{T}$ with their compound matrices of order 2 (Pestel and Leckie, 1963). The order-2 compound matrix of a given matrix $\mathbf{X}$ (denoted $\overline{\mathbf{X}}$) is built from all the order-2 minors of $\mathbf{X}$, and grouped in order. This transformation, known also as the Delta-matrix method, does not affect the characteristic function. For a better numerical efficiency, I calculated the analytical expressions of the necessary $6\times6$ compound matrices $\overline{\mathbf{E}}$, $\overline{\mathbf{Q}}$, $\overline{\mathbf{Q}^{-1}}$, and $\overline{\mathbf{T}}$ while taking into account symmetry and common factors whenever they appear. I give in a supplementary document the entries of these compound matrices.

*Root finding and curve tracing*

I follow the procedure proposed by Lowe (1995) to trace the normal modes dispersion curves. Starting from a given $(f, k)$ or $(f, c)$ root, I take small regular steps in frequency and find for each the corresponding root close to an initial guess. I compute the initial guess by extrapolating previous roots. In order to handle crossing curves robustly, I use previous roots in an alternate fashion to perform the extrapolation. I compute the starting root for each curve by wavenumber or phase velocity sweep. The implementation for leaky modes is significantly more evolved as it requires finding the roots of a complex valued function depending on three variables, but the general procedure remains the same.

# APPENDIX A

# MATRIX COEFFICIENTS FOR LAYERED MEDIA

The entries of the elementary matrices in the Thomson-Haskell method are given below:

$$\mathbf{W} = ke^{i(kx-\omega t)} \begin{pmatrix} i & & & \\ & i & & \\ & & k & \\ & & & k \end{pmatrix}$$

$$\mathbf{E} = \begin{pmatrix} e^{ikr_a z} & & & \\ & e^{-ikr_a z} & & \\ & & e^{ikr_b z} & \\ & & & e^{-ikr_b z} \end{pmatrix}$$

$$\mathbf{Q} = \begin{pmatrix} 1 & 1 & -r_b & r_b \\ r_a & -r_a & 1 & 1 \\ -2\mu r_a & 2\mu r_a & -\mu t & -\mu t \\ \mu t & \mu t & -2\mu r_b & 2\mu r_b \end{pmatrix}$$

$$\mathbf{Q}^{-1} = \begin{pmatrix} \gamma & -\frac{2\gamma-1}{2r_a} & -\frac{\gamma}{2\mu r_a} & -\frac{\gamma}{2\mu} \\ \gamma & \frac{2\gamma-1}{2r_a} & \frac{\gamma}{2\mu r_a} & -\frac{\gamma}{2\mu} \\ \frac{2\gamma-1}{2r_b} & \gamma & \frac{\gamma}{2\mu} & -\frac{\gamma}{2\mu r_b} \\ -\frac{2\gamma-1}{2r_b} & \gamma & \frac{\gamma}{2\mu} & \frac{\gamma}{2\mu r_b} \end{pmatrix}$$

$$T_{11} = \gamma(2C_a - tC_b)$$

$$T_{12} = -i\gamma(\frac{t}{r_a}S_a + 2r_b S_b) \qquad T_{31} = -i\gamma\mu(4r_a S_a + \frac{t^2}{r_b}S_b)$$

$$T_{13} = -i\frac{\gamma}{\mu}(\frac{1}{r_a}S_a + r_b S_b) \qquad T_{32} = 2\gamma\mu t(C_a - C_b)$$

$$T_{14} = -\frac{\gamma}{\mu}(C_a - C_b) \qquad T_{33} = T_{11}$$

$$T_{21} = i\gamma(2r_a S_a + \frac{t}{r_b}S_b) \qquad T_{34} = T_{21}$$

$$T_{22} = -\gamma(tC_a - 2C_b) \qquad T_{41} = T_{32}$$

$$T_{23} = T_{14} \qquad T_{42} = -i\gamma\mu(\frac{t^2}{r_a}S_a + 4r_b S_b)$$

$$T_{24} = -i\frac{\gamma}{\mu}(r_a S_a + \frac{1}{r_b}S_b) \qquad T_{43} = T_{12}$$

$$T_{44} = T_{22}$$

with the following notations:

$$
\begin{aligned}
C_a &= \cos(kr_a z) \\
C_b &= \cos(kr_b z) \\
S_a &= \sin(kr_a z) \\
S_b &= \sin(kr_b z) \\
\mu &= \rho\beta^2 \\
\gamma &= \frac{\beta^2}{c^2} \\
t &= 2 - \frac{c^2}{\beta^2}
\end{aligned}
$$

## REFERENCES


Aki, K., and P. G. Richards, 2002, Quantitative seismology.

Boiero, D., E. Wiarda, and P. Vermeer, 2013, Surface-and guided-wave inversion for near-surface modeling in land and shallow marine seismic data: The Leading Edge, **32**, 638–646.

Buchen, P., and R. Ben-Hador, 1996, Free-mode surface-wave computations: Geophysical Journal International, **124**, 869–887.

Haskell, N. A., 1953, The dispersion of surface waves on multilayered media: Bulletin of the seismological Society of America, **43**, 17–34.

Hou, S., R. Haacke, A. Corbett, and M. Wanczuk, 2018, Velocity model building with guided wave inversion: 80th EAGE Conference and Exhibition 2018, European Association of Geoscientists & Engineers, 1–5.

Krey, T. C., 1963, Channel waves as a tool of applied geophysics in coal mining: Geophysics, **28**, 701–714.

Lamb, H., 1917, On waves in an elastic plate: Proceedings of the Royal Society of London. Series A, Containing papers of a mathematical and physical character, **93**, 114–128.

Li, J., S. Hanafy, and G. Schuster, 2018, Wave-Equation Dispersion Inversion of Guided P Waves in a Waveguide of Arbitrary Geometry: Journal of Geophysical Research: Solid Earth, **123**, 7760–7774.

Lowe, M. J., 1995, Matrix techniques for modeling ultrasonic waves in multilayered media: IEEE transactions on ultrasonics, ferroelectrics, and frequency control, **42**, 525–542.

Pestel, E., and F. A. Leckie, 1963, Matrix methods in elastomechanics: McGraw-Hill.

Rao, J., M. Ratassepp, and Z. Fan, 2016, Guided wave tomography based on full waveform inversion: IEEE transactions on ultrasonics, ferroelectrics, and frequency control, **63**, 737–745.

Ryden, N., and M. J. Lowe, 2004, Guided wave propagation in three-layer pavement structures: The Journal of the Acoustical Society of America, **116**, 2902–2913.

Thomson, W. T., 1950, Transmission of elastic waves through a stratified solid medium: Journal of applied Physics, **21**, 89–93.

Vallet, Q., N. Bochud, C. Chappard, P. Laugier, and J.-G. Minonzio, 2016, In vivo characterization of cortical bone using guided waves measured by axial transmission: IEEE transactions on ultrasonics, ferroelectrics, and frequency control, **63**, 1361–1371.

Viktorov, I., 1967, Rayleigh and Lamb waves: Physical Theory and Applications: Plenum, New York.